

# Stretching of viscous threads at low Reynolds numbers

By **JONATHAN J. WYLIE**<sup>1,2</sup>, **HUAXIONG HUANG**<sup>2,3</sup>  
AND **ROBERT M. MIURA**<sup>2,4</sup>

<sup>1</sup>Department of Mathematics, City University of Hong Kong, Kowloon, Hong Kong.

<sup>2</sup>Center for Applied Mathematics and Statistics, New Jersey Institute of Technology, Newark,  
NJ 07102 USA.

<sup>3</sup>Department Mathematics and Statistics, York University, Toronto, Ontario, Canada M3J  
1P3.

<sup>4</sup>Department of Mathematical Sciences, New Jersey Institute of Technology, Newark, NJ  
07102, USA.

(Received ?? and in revised form ??)

We investigate the classical problem of the extension of an axisymmetric viscous thread by a fixed applied force with small initial inertia and small initial surface tension forces. We show that inertia is fundamental in controlling the dynamics of the stretching process. Under a long-wavelength approximation, we derive leading-order asymptotic expressions for the solution of the full initial-boundary value problem for arbitrary initial shape. If inertia is completely neglected, the total extension of the thread tends to infinity as the time of pinching is approached. On the other hand, the solution exhibits pinching with finite extension for any non-zero Reynolds number. The solution also has the property that inertia eventually must become important, and pinching must occur at the pulled end. In particular, pinching cannot occur in the interior as can happen when inertia is neglected. Moreover, we derive an asymptotic expression for the extension.

---

## 1. Introduction

In this paper, we consider an axisymmetric viscous thread that is pulled at its ends by an imposed fixed force. This type of extensional viscous flow is crucial to a number of industrial applications. An important example is the production of glass fibers for optical microscopy (Gallacchi *et al.*, 2001), where glass is extended to form highly tapered microscope tips. This type of flow is also critical in the manufacture of glass microelectrodes (Huang *et al.*, 2003 and Huang *et al.*, 2007), where a glass tube is pulled to form an electrode that is sufficiently sharp and thin to pierce the membranes of biological cells. Flows of this type also form the basis of devices that measure extensional viscosity (Matta & Tytus 1990).

There exists an extensive literature on the localized pinching behaviour of thin liquid threads, and we refer the reader to the review article by Eggers (2005) and the references therein for further details. In much of the previous work, the focus has been to determine the dynamics of pinching and they have typically not been concerned with the complete initial-boundary value problem. The local pinching solution has been shown to be universal, but the location and time of pinching can only be determined by considering the initial and boundary conditions. On the other hand, the problem of a filament evolving from its initial condition has received much less attention. Indeed, the question of what initial conditions can lead to the universal pinching solution remains an open question. In this paper, we will derive analytical solutions of the long-wavelength equations that are valid for the full initial-boundary value problem at initially low Reynolds numbers.

As mentioned above, there has been much less work on the evolution of threads from an initial configuration and how the initial configuration affects the nature of the ultimate pinching behaviour. Wilson (1988) and Stokes *et al.* (2000) have considered the full initial-boundary value problem for filaments that are stretched by gravity when inertia

can be completely neglected. When inertia is neglected, the filament can pinch and the acceleration of the filament can become infinite in a finite time. The large accelerations imply that inertia must ultimately become important. Huang *et al.* (2003) and Huang *et al.* (2007) neglected inertia and considered the stretching of heated viscous filaments with temperature-dependent viscosity. Wylie & Huang (2007) showed that viscous heating and inertia effects can become important as one approaches pinching and that these effects can dramatically affect the flow. Kaye (1991) considered extensional flows with inertia, but did not discuss the role of inertia in cases in which the accelerations become large. A number of authors have used numerical methods to attack initial-boundary value problems for stretched threads when inertia is included. Stokes & Tuck (2004) used a numerical method to solve the full initial-boundary value problem, including inertia, for a filament stretched by gravity. They numerically showed that inertia becomes important when the filament becomes sufficiently stretched. In particular, they showed that the solution has large gradients and this causes numerous numerical difficulties that require sophisticated numerical methods. Bradshaw-Hajek *et al.* (2007) developed such a method and gave a good discussion of the challenges in obtaining accurate solutions when the filament becomes very heavily extended.

All of these studies mentioned in the above paragraph have neglected surface tension effects and Stokes & Tuck (2004) posed the important question: for what initial conditions do surface tension effects become important for such flows? Numerically, one can readily study flows with moderately low Reynolds number. However, for the very low Reynolds numbers that frequently occur in practice, resolving the regions where there are large gradients is difficult. Therefore, an asymptotic theory that is valid for low Reynolds numbers would be extremely valuable in obtaining the solution. Furthermore, it would provide a detailed understanding of the mechanics that occur in the various regions of

the flow, particularly those regions with large gradients. Moreover, such a theory would be able to provide answers to the questions of whether and when surface tension effects become important.

Despite the extensive numerical work on this problem, there has been little analytical progress when inertial effects are included. In this paper, for low Reynolds numbers, we derive asymptotic solutions to the long-wavelength equations for the problem of a viscous thread that is pulled at its ends by an imposed fixed force. We will show that if inertia is neglected, the thread can pinch either at a pulled end or in the interior. As one approaches pinching, the total extension becomes infinite. However, if inertia is included, the solutions have the property that the thread must pinch at one of the pulled ends. Moreover, the extension of the thread must be finite at pinching. We describe the mechanism by which inertia prevents pinching in the interior and derive asymptotic expressions for the resulting shape of the thread.

## 2. Formulation

We consider an axisymmetric viscous thread that is pulled at its ends by a fixed force  $F$ . The thread is composed of a Newtonian fluid with density  $\rho$ , surface tension coefficient  $\gamma$ , and viscosity  $\mu$ . We denote time by  $t$  and the distance along the thread measured from the center of mass by  $x$ . The cross-sectional area of the thread is denoted by  $A(x, t)$ , and its initial values are given by  $A_0(x)$ . The two end points of the thread are initially located at  $x = L_+$  and  $x = L_-$  where  $L_- < 0 < L_+$ . We will assume that  $L_+$  and  $L_-$  are of the same order of magnitude and use  $L_+$  for non-dimensionalization.

### 2.1. Eulerian Formulation

We define the minimum of the initial cross-sectional area to be  $A_{min} \equiv \min_x A_0(x)$  and define the aspect ratio to be  $\delta = A_{min}/L_+^2$ . For small aspect ratio,  $\delta \ll 1$ , the

governing equations for laminar, axisymmetric, and incompressible extensional flow have been derived by a number of authors (for example, see Fitt *et al.*, 2000; Forest *et al.* 2000; and Yin & Jaluria, 2000 for detailed derivations). These authors have shown that, to leading order in the aspect ratio, the axial velocity of the fluid is independent of the radial coordinate. Thus, we denote the axial velocity by  $U(x, t)$ . Using a nondimensionalisation given by

$$U = \frac{FL_+}{3\mu A_{min}} U', \quad A = A_{min} A', \quad A_0 = A_{min} A'_0, \quad x = L_+ x', \quad \text{and} \quad t = \frac{3\mu A_{min}}{F} t',$$

and dropping the primes, the governing equations take the form

$$A_t + (UA)_x = 0, \tag{2.1}$$

$$R(U_t + UU_x) = \frac{1}{A} \left( AU_x + \lambda A^{1/2} \right)_x, \tag{2.2}$$

where

$$R = \frac{\rho FL_+^2}{9\mu^2 A_{min}} \quad \text{and} \quad \lambda = \frac{\gamma \sqrt{\pi A_{min}}}{F}.$$

Equations (2.1) and (2.2) represent the conservation of mass and momentum, respectively. The dimensionless quantity  $R$  is the Reynolds number based on the initial length of the thread and the initial velocity scale  $FL_+(\mu A)$  that balances the viscous force and the imposed force. The dimensionless quantity  $\lambda$  is a measure of the surface tension force relative to the imposed force.

The initial conditions are given by

$$U = 0 \quad \text{and} \quad A = A_0(x) \quad \text{at} \quad t = 0. \tag{2.3}$$

The boundary conditions at the two end points of the thread are constant extensional forces, that is,

$$AU_x + \lambda A^{1/2} = 1 \quad \text{at} \quad x = \ell_{\pm}(t) \tag{2.4}$$

where  $\ell_+(t)$  and  $\ell_-(t)$  are the dimensionless locations of the right- and left-hand ends of

the thread, respectively, at which the fixed forces are applied. The functions  $\ell_+(t)$  and  $\ell_-(t)$  are obtained by solving the ordinary differential equations that correspond to the kinematic conditions at the end points,

$$\frac{d\ell_{\pm}}{dt} = U(\ell_{\pm}(t), t) \quad (2.5)$$

subject to the initial conditions  $\ell_+(0) = 1$  and  $\ell_-(0) = L_-/L_+$ .

## 2.2. Lagrangian Formulation

Stokes & Tuck (2004) and Wylie & Huang (2007) showed that the system of equations (2.1)-(2.4) becomes significantly simpler if expressed in Lagrangian coordinates. In this paper, we use a different Lagrangian transformation that transforms the equations into a particularly simple form. We transform from the Eulerian variables  $(x, t)$  to scaled Lagrangian variables  $(\xi, \tau)$ . We define  $\tau = t$  and  $\xi$  is defined implicitly by

$$\xi = \frac{\int_0^{X(\xi, 0)} A_0(x') dx'}{\int_0^1 A_0(x') dx'} \quad (2.6)$$

where  $X(\xi, \tau)$  is the spatial coordinate of a material element at time  $\tau$ . The Lagrangian variable,  $\xi$ , labels each fluid element in terms of its initial location. Fluid elements travel with the fluid velocity and so  $U = X_{\tau}$ . We note that  $|\xi|$  represents the initial volume of the fluid between zero and  $x$  divided by the total initial volume of the thread in the region  $0 \leq x \leq 1$ . Under this transformation, the two ends of the thread are located at  $\xi = 1$  and  $\xi = \xi_-$  where

$$\xi_- = \frac{\int_0^{L_-/L_+} A_0(x') dx'}{\int_0^1 A_0(x') dx'}.$$

In the scaled Lagrangian coordinates, we denote  $s(\xi, \tau) = A(x, t)$ ,  $s_0(\xi) = A_0(x)$ , and  $v(\xi, \tau) = U(x, t)$ . The partial derivatives in the Lagrangian coordinates are given by

$$\frac{\partial}{\partial \tau} = \frac{\partial}{\partial t} + \frac{\partial X}{\partial \tau} \frac{\partial}{\partial x} = \frac{\partial}{\partial t} + U \frac{\partial}{\partial x} \quad (2.7)$$

$$\frac{\partial}{\partial \xi} = \frac{\partial X}{\partial \xi} \frac{\partial}{\partial x}. \quad (2.8)$$

Then, the equation for the conservation of mass (2.1) becomes

$$\frac{\partial s}{\partial \tau} + \frac{s}{\partial X / \partial \xi} \frac{\partial U}{\partial \xi} = 0. \quad (2.9)$$

Multiplying by  $\partial X / \partial \xi$  and substituting  $U = \partial X / \partial \tau$ , we obtain

$$\frac{\partial}{\partial \tau} \left( s \frac{\partial X}{\partial \xi} \right) = 0. \quad (2.10)$$

Equation (2.10) implies that  $sX_\xi$  is a function of  $\xi$  only. This function can be determined by using the initial conditions  $s(\xi, 0) = s_0(\xi)$  and (2.6). Differentiating (2.6) with respect to  $\xi$  gives  $X_\xi(\xi, 0) = I/s_0(\xi)$ , and so we obtain

$$sX_\xi = I \quad (2.11)$$

where

$$I = \int_0^1 A_0(x') dx'. \quad (2.12)$$

This allows us to compute the location  $X$  of a material point at time  $\tau$  that was initially at position,  $\xi$ , namely

$$X(\xi, \tau) = I \int_0^\xi \frac{1}{s(y, \tau)} dy. \quad (2.13)$$

Thus, in Lagrangian coordinates, the equations for mass (2.1) and momentum (2.2) become

$$Is_\tau = -s^2 v_{\xi, \xi}, \quad (2.14)$$

$$I^2 R v_\tau = \left[ s^2 v_\xi + I \lambda s^{1/2} \right]_{\xi\xi}. \quad (2.15)$$

Cross-differentiating (2.14) and (2.15) to eliminate terms involving  $v$ , we obtain a single equation for  $s$  given by

$$\tilde{R} \left[ \frac{s_\tau}{s^2} \right]_\tau = \left[ s_\tau - \lambda s^{1/2} \right]_{\xi\xi\xi} \quad (2.16)$$

where

$$\tilde{R} \equiv I^2 R. \quad (2.17)$$

The equation (2.16) requires two initial conditions on  $s$ . The first is given by the initial profile

$$s(\xi, 0) = s_0(\xi). \quad (2.18)$$

The second can be derived from the conditions  $v(\xi, 0) = 0$  and the conservation of mass (2.14) and is given by

$$s_\tau(\xi, 0) = 0. \quad (2.19)$$

The equation (2.16) also requires two boundary conditions, which can be derived from (2.4) and (2.14) and are given by

$$s_\tau = -1 + \lambda s^{1/2} \quad \text{at} \quad \xi = 1 \quad \text{and} \quad \xi = \xi_-. \quad (2.20)$$

The parameter values can vary widely depending on the particular application. Here, we give order of magnitude estimates that are appropriate for electrode pulling. These parameter values are  $L_+ \sim 10^{-2}$  m,  $A_{min} \sim 10^{-6}$  m,  $F \sim 1$  N,  $\rho \sim 10^3$  kg/m<sup>3</sup>,  $\gamma \sim 10^{-1}$  kg/s<sup>2</sup>, and  $\mu \sim 10^4$  kg/m/s (Gallacchi *et al.*, 2001 and Huang *et al.*, 2003). These parameter values lead to the following estimates of the dimensionless parameters:  $\delta \sim 10^{-2}$ ,  $R \sim 10^{-4}$ , and  $\lambda \sim 10^{-4}$ .

Based on these estimates, the inertia and surface tension terms are small. These facts have led many authors to neglect both of these effects. However, one must remember that these estimates are based on the characteristic scales that may not be appropriate if the filament becomes thin or if large gradients develop. We will show that this is exactly what happens in this problem. When the filament becomes sufficiently thin, the inertial terms become important and one must retain the terms involving  $R$ . On the other hand, we will show that the surface tension terms do not become important as the thread becomes stretched, and we therefore neglect the surface tension terms by setting  $\lambda = 0$ .

In fact, proving the validity of neglecting the surface tension term is nontrivial and will be discussed in detail in Section 7.

Setting  $\lambda = 0$  in (2.16), integrating with respect to time, and using the initial conditions (2.18) and (2.19), we obtain

$$\tilde{R}s_\tau = -s^2(s_0 - s)_{\xi\xi}. \quad (2.21)$$

We note that (2.21) is a nonlinear diffusion equation that becomes degenerate when the cross-sectional area of the thread is zero, that is,  $s = 0$ . An equation similar to (2.21) was derived by Stokes & Tuck (2004) for a drop extending under gravity, but in their case, the boundary conditions are different from those considered here.

Using the initial condition (2.18), the boundary conditions (2.20) can be integrated with respect to time to yield

$$s = s_0 - \tau \quad \text{at} \quad \xi = 1 \quad \text{and} \quad \xi = \xi_-. \quad (2.22)$$

According to this boundary condition, a pinching event, in which the cross-sectional area  $s$  becomes zero, must either occur at an end point at  $\tau = \min\{s_0(1), s_0(\xi_-)\}$  or at an interior point at an earlier time. For zero Reynolds number, we will show that the thread can pinch at an interior point, but for any non-zero Reynolds number, the thread must pinch at an end point.

We conclude this section by noting that (2.21), (2.18), and (2.22) form a closed system of equations.

### 3. Pinching without Inertia

In this section, we consider the problem when  $\tilde{R} = 0$ , that is, when inertia is neglected. We will discuss the effects of inertia in Section 6. In this case, the system can be readily

solved to give

$$s(\xi, \tau) = s_0(\xi) - \tau. \quad (3.1)$$

By definition,  $\min_{\xi} s_0(\xi) \equiv 1$  and so the cross-sectional area is zero and the thread pinches at time  $\tau = 1$ . We define the value of  $\xi$  at which the minimum, and hence the pinching, occurs at  $\xi_{min} = \operatorname{argmin}_{\xi} s_0(\xi)$ . Without loss of generality, we assume that  $\xi_{min} \geq 0$ .

In order to determine the physical location of the fluid elements denoted by  $\xi$ , one must evaluate the extension integral (2.13) to get

$$X(\xi, \tau) = I \int_0^{\xi} \frac{1}{s_0(y) - \tau} dy. \quad (3.2)$$

### 3.1. Initial minimum located at end point

We begin with the case in which the initial minimum occurs at the end point, that is  $\xi_{min} = 1$ . We note that  $s_{0\xi}(1) \leq 0$  since  $\xi = 1$  is a minimum. In the generic case,  $s_{0\xi}(1) < 0$ , the integral (3.2) that determines the location of the end point is dominated by the contribution near  $\xi = 1$  as  $\tau \rightarrow 1$ . This is given by

$$X(1, \tau) \sim I \int_0^1 \frac{1}{1 - \tau + s_{0\xi}(1)(y - \xi_{min})} dy \quad (3.3)$$

$$\sim \frac{I}{s_{0\xi}(1)} \ln(1 - \tau). \quad (3.4)$$

In the non-generic case,  $s_{0\xi}(1) = 0$  and  $s_{0\xi\xi}(1) > 0$ , a similar calculation yields  $X(\xi, \tau) = O((1 - \tau)^{-1/2})$ .

### 3.2. Initial minimum located away from end points

We now consider the case in which the minimum is not located at the end point, that is  $0 \leq \xi_{min} < 1$ , and assume that the initial profile is twice differentiable. Then, since  $\xi_{min}$  is a minimum, we have  $s_{0\xi}(\xi_{min}) = 0$  and  $s_{0\xi\xi}(\xi_{min}) \geq 0$ . If  $\xi > \xi_{min}$ , then, as  $\tau \rightarrow 1$ , the integral (3.2) is dominated by the contribution near  $\xi_{min}$ . We first consider

the generic case in which  $s_{0\xi\xi}(\xi_{min}) > 0$ . We obtain

$$X(\xi, \tau) \sim I \int_0^\xi \frac{1}{1 - \tau + \frac{1}{2}s_{0\xi\xi}(\xi_{min})(y - \xi_{min})^2} dy \quad (3.5)$$

$$\sim \begin{cases} I\pi \sqrt{\frac{2}{s_{0\xi\xi}(\xi_{min})(1-\tau)}} & \text{if } \xi_{min} > 0 \\ \frac{I\pi}{2} \sqrt{\frac{2}{s_{0\xi\xi}(\xi_{min})(1-\tau)}} & \text{if } \xi_{min} = 0 \end{cases}$$

for  $\tau \rightarrow 1$ . In the non-generic case in which  $s_{0\xi\xi}(\xi_{min}) = 0$ , the third derivative must be zero because  $\xi_{min}$  is a local minimum, but if the fourth derivative is non-zero, then a similar calculation shows that  $X(\xi, \tau) = O((1 - \tau)^{-3/4})$ .

In all cases, the total extension tends to infinity as  $\tau \rightarrow 1$ . This implies that the velocities also tend to infinity, and therefore, neglecting the inertial terms cannot remain valid as  $\tau \rightarrow 1$ . In the following sections we will investigate the effect of inertia.

#### 4. Stretching with Inertia: Numerical Examples

Although the governing system appears to be simple, we will show that this problem poses numerous theoretical and computational challenges that are not at all obvious at the outset. Before introducing our theoretical analysis, we will present the results of numerical computations to give the reader a flavour of the complexity that can arise.

We consider two initial shapes that are superficially similar, but lead to surprisingly different behaviour (see the dashed lines in Figures 1a and b. In both figures, the initial shape has two local minima  $0 < \xi_1 < \xi_2 < 1$  and both curves are symmetric about  $\xi = 0$ . The difference between the two initial shapes is that in the first case,  $\xi_2$  is the global minimum and in the second case  $\xi_1$  is the global minimum. Computationally, it is more convenient to solve the problem using Lagrangian variables. We spatially discretize (2.21) with a second-order central-difference formula and solve the resulting system of ordinary differential equations using a standard numerical ODE solver. The computations were performed for  $\tilde{R} = 10^{-2}$ .

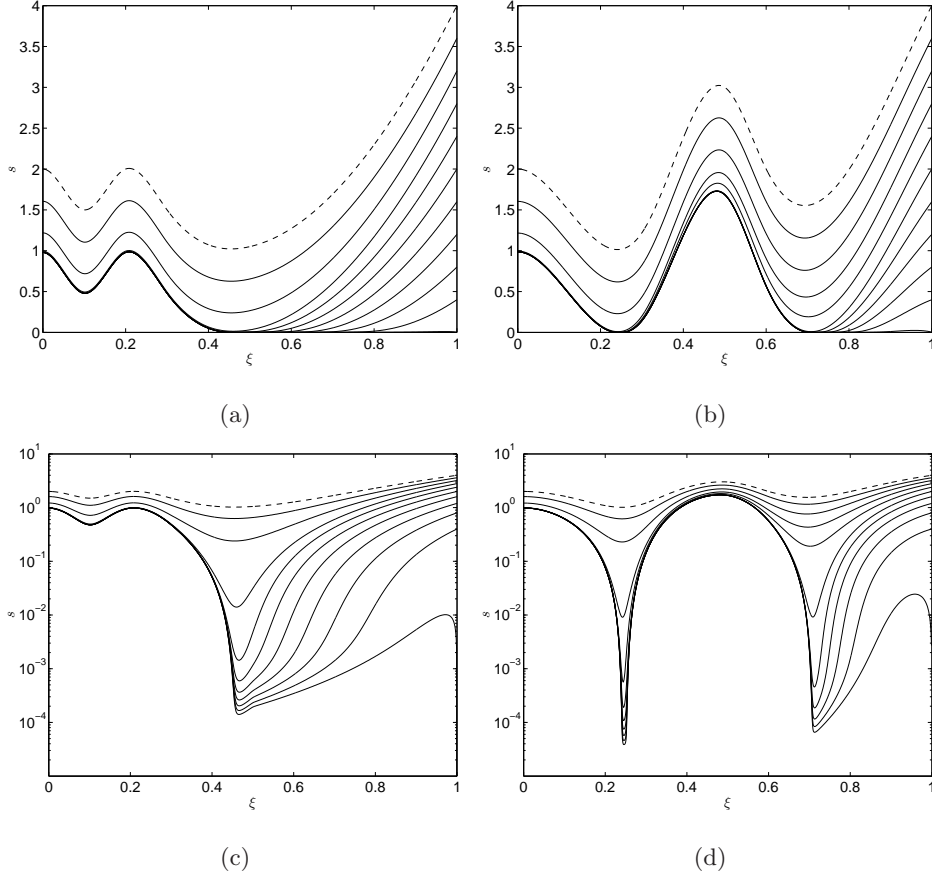


FIGURE 1. The cross-sectional area is plotted against the Lagrangian variable,  $\xi$  for  $\tilde{R} = 0.01$ . The dashed line is the initial shape and the solid lines are the shape at various times  $\tau=0.4, 0.8, \dots, 4$ . Figures (a) and (b) have linear scales; Figures (c) and (d) have logarithmic scales.

Figure 1a shows the cross-sectional area at various times for the first initial shape. In the early stages, the thread thins uniformly until the cross-sectional area at  $\xi_2$  becomes small. Beyond this time, only the region to the right of  $\xi_2$  experiences significant thinning. Ultimately, the thread pinches at the pulled end  $\xi = 1$ . In order to appreciate the degree of thinning in different regions, we also plot the cross-sectional areas on a logarithmic scale in Figure 1c. It is clear that the region near  $\xi_2$  experiences much more dramatic thinning than the region near  $\xi_1$ . We also note that the pinching at the pulled end is highly localized.

Figure 1b shows the results for the second initial shape. In the early stages, the thread thins uniformly until the cross-sectional area at  $\xi_1$  becomes small. Beyond this time, the only significant thinning that occurs is in the region  $\xi > \xi_1$ . This continues until a critical time at which the cross-sectional area near  $\xi_2$  becomes small. Beyond this time, only the region to the right of  $\xi_2$  experiences significant thinning. Again, the thread pinches at the pulled end  $\xi = 1$ . Figure 1d shows the results on a logarithmic scale. It can be seen that the thread thins dramatically in the regions close to both  $\xi_1$  and  $\xi_2$ . This is in contrast to the previous case, in which only the region near  $\xi_2$  experiences significant thinning.

Although it is convenient to use Lagrangian coordinates for computational purposes, from a physical point of view, it is crucial to express the solution in Eulerian coordinates. In Figure 2, we plot the cross-sectional areas in Eulerian co-ordinates at a time when substantial thinning has occurred. They show that for both of the two initial shapes, the thread extends dramatically as it thins and the vast majority of the length corresponds to the necking regions. Figure 2a shows that the necking region that corresponds to the initial minimum at  $\xi_2$  has extended to a length of almost 1000, whereas the outer regions occupy very small lengths near  $x = 0$  and at the pulled end. These regions are shown in the figure inserts. Figure 2b shows the case with two necking regions. The necking region that corresponds to the initial minimum at  $\xi_1$  occupies most of the length from  $x = 0$  to more than 400, while the necking region that corresponds to the initial minimum at  $\xi_2$  occupies most of the remaining length. The three regions in which  $A$  is not small occupy only small lengths near  $x = 0, 423,$  and  $1190$ . The results are also plotted on a logarithmic scale in Figures 2c and d so that the extent of the thinning is clear.

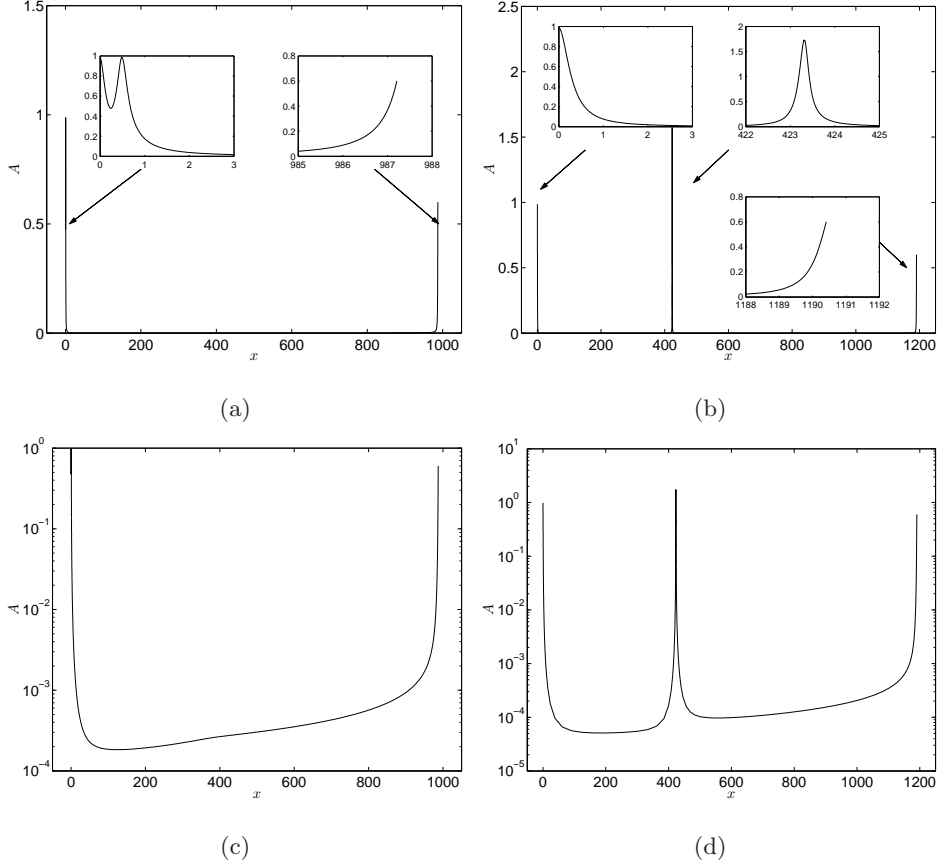


FIGURE 2. The cross-sectional area is plotted against the Eulerian variable,  $x$ . Figures (a) and (c) correspond to the initial condition shown in Figure 1(a) and Figures (b) and (d) correspond to the initial condition shown in Figure 1(b). Figures (a) and (b) have linear scales; Figures (c) and (d) have logarithmic scales. The time is  $\tau = 3.4$  and  $\tilde{R} = 0.01$ .

## 5. Stretching with Inertia: Obstacle Problem

Later in this paper, we will use a formal procedure to derive the asymptotic solution that is valid for low Reynolds number. Before presenting the formal asymptotic method, we give an informal geometric argument that converts the leading-order problem into a simple ‘obstacle problem’. This informal procedure is significantly simpler than the formal asymptotic matching. In addition, it sheds significant light on the asymptotic solution.

If  $\tilde{R} \ll 1$  and we consider regions in which  $s = O(1)$ , then the inertial term in (2.21)

is negligible. Putting  $\tilde{R} = 0$  in (2.21), we see that  $s^2(s - s_0)_{\xi\xi} = 0$ . As long as  $s$  remains  $O(1)$ , we have  $s_{\xi\xi} = s_0\xi\xi$ . This implies that  $s_0 - s$  must be a linear function of  $\xi$ . We will refer to these regions as “outer regions”.

On the other hand, if  $\tilde{R} \ll 1$ , it is also possible to find solutions to (2.21) in regions in which  $s$  is small. To see this, it is instructive to rewrite (2.21) in the form

$$\tilde{R} \left( \frac{1}{s} \right)_{\tau} = (s_0 - s)_{\xi\xi}. \quad (5.1)$$

If  $s$  is small, we can approximate  $s_0 - s$  on the right-hand side of (5.1) by  $s_0$  and obtain

$$\tilde{R} \left( \frac{1}{s} \right)_{\tau} = s_0\xi\xi. \quad (5.2)$$

This indicates that there may be regions where  $s = O(\tilde{R})$ . We will refer to these regions as “necking regions”.

To show that this problem can be viewed as a simple obstacle problem, we use  $s_0 - s$  as a new variable that represents the deviation from the initial shape. Using this variable, there are two basic types of solutions. In the necking regions,  $s_0 - s$  is approximately  $s_0$  and in the outer regions  $s_0 - s$  is a linear function of  $\xi$ . For  $\tilde{R} \ll 1$ , we can patch together the two types of solutions to construct the complete solution. When patching together a necking region with an outer region, we must satisfy matching conditions at the interface between the two regions. These can be derived by considering a standard argument regarding the continuity of the flux,  $(s_0 - s)_{\xi}$ , in (5.1). This implies that  $s_0 - s$  and its derivative must be continuous at the interface between the two regions. Therefore, given appropriate boundary conditions, these matching conditions imply that a unique solution can be obtained.

The leading-order problem in the variable  $s_0 - s$  can be thought of as an obstacle problem with an elastic string whose end moves with time. Since  $s \geq 0$ , the largest value that  $s_0 - s$  can attain is  $s_0$  and thus the obstacle is given by  $s_0 - s$  equals  $s_0$ . The necking

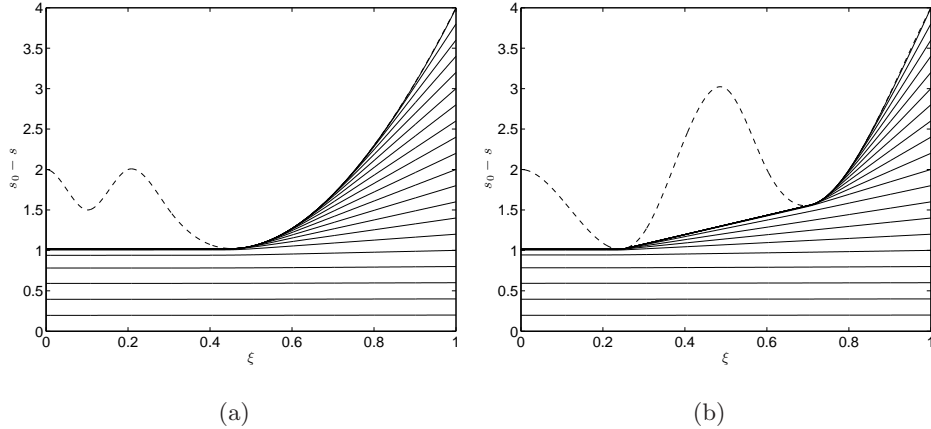


FIGURE 3. Departure from the initial cross-sectional area for  $\tilde{R} = 0.01$  at various times:  $\tau=0, 0.2, \dots, 4$ . Figures (a) and (b) correspond to two different initial shapes, as indicated by the dashed lines.

regions correspond to the regions in which the string is in contact with the object. The outer regions correspond to the regions in which the string is not in contact with the object and are made up of straight lines.

In Figure 3, we replot the numerical solutions obtained earlier using the new variable  $s_0 - s$  to show how these solutions can be interpreted as solutions of obstacle problems. We also plot the initial profile  $s_0$  that represents the obstacle. We note that using the new variable  $s_0 - s$ , the boundary condition (2.22) takes the form  $s_0 - s = \tau$  at  $\xi = 1$ . If the thread is symmetric, then we also have the symmetry condition  $\partial_\xi(s_0 - s) = 0$  at  $\xi = 0$ .

In Figures 3a and b, we see that when  $\tau < 1$ , there is no necking region and only an outer-region solution given by  $s_0 - s = \tau$ . This is the same as the inertialess solution obtained in Section 3. For  $\tau > 1$ , it is no longer possible to construct a solution in the form of a linear function of  $\xi$  that satisfies both of the boundary conditions. In this case, one must patch together necking and outer regions to obtain the solution.

We now illustrate how this is done with the two examples. We begin with Figure 3a

in which only a single necking region can ever occur. The location of the left end of the necking region must be obtained by matching the value and gradient with the outer region. In this case, the symmetry condition  $\partial_\xi(s_0 - s) = 0$  at  $\xi = 0$  implies that the outer solution must be a horizontal line and thus contact with the obstacle with zero slope. Hence, the solution to the left of the necking region is given by  $s_0 - s = 1$  and the location of the left end of the necking region is given by  $\xi = \xi_2$  and does not vary with time. We also see that the right end of the necking region moves to the right as time progresses. To determine the location of the right end of the necking region (which we denote by  $\xi_c(\tau)$ ) one must match the value and gradient with the outer region. The straight line that satisfies the boundary condition  $s_0 - s = \tau$  at  $\xi = 1$  and is tangent to the obstacle at  $\xi_c$  is given by

$$s_0 - s = \tau + (\xi - 1)s_{0\xi}(\xi_c). \quad (5.3)$$

The condition that determines  $\xi_c$  is given by the property that the straight line must connect with the obstacle

$$s_0(\xi_c) = \tau + (\xi_c - 1)s_{0\xi}(\xi_c). \quad (5.4)$$

Eventually, the necking region extends all the way to  $\xi = 1$ , and at this time, the thread pinches at  $\xi = 1$ .

In Figure 3b, the situation is different and two necking regions can form, but a similar approach can still be used. For  $\tau > 1$ , but less than a critical value, there is only a single necking region whose left end is fixed at  $\xi = \xi_1$  and whose right end moves with time in a similar way to that in Figure 3a. For  $\tau$  greater than the critical value, another necking region forms. The left end of the new necking region is fixed and is given by finding the common tangent line with the obstacle. For times beyond the critical time, the location of the original necking region does not change. As in the previous case, the

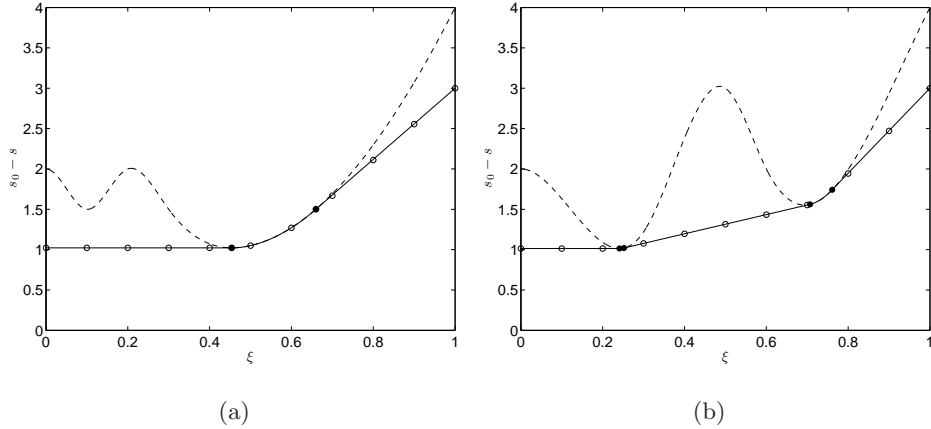


FIGURE 4. Comparison between solution of the obstacle problem (solid line) and the numerical solution (open circles) for the departure from the initial cross-sectional area. The solid circles represent the boundaries between the necking and outer regions. The time is  $\tau=3$  and  $\tilde{R} = 0.01$ . Figures (a) and (b) correspond to the two different initial shapes, indicated by the dashed lines.

thread ultimately pinches when the right end of the new necking region coincides with  $\xi = 1$ .

This reformulation as an obstacle problem represents a significant simplification because solving the obstacle problem is a purely geometric exercise. In Figure 4, we plot the comparison between the solution of the obstacle problem and the numerical solution for the two initial shapes. It can be seen that the agreement between the two is excellent.

The solution to the obstacle problem provides us with a significant amount of useful information about the solution in the Lagrangian variables. However, it cannot be compared directly with the numerical solution in Eulerian coordinates, which is more important physically. This is because, in order to convert to the Eulerian coordinates one needs to evaluate the extension integral (2.13). The obstacle problem provides the leading-order information about  $s$ . In the necking region, the leading-order solution to the obstacle problem is zero. Since  $s$  is the denominator of the integrand, one needs to know the size of  $s$  in the necking region. In order to achieve this, we will use a formal

asymptotic procedure to obtain the solution beyond the leading order. This procedure also re-derives the matching conditions between necking and outer regions in a more formal manner. This informal method of patching is not conducive to determining the sizes of the asymptotic corrections. These quantities will be derived using the formal asymptotic procedure in the following section.

## 6. Stretching with Inertia: Formal Asymptotics

In this section, we first derive the corrections to the inertialess solution for the generic problem. This is given in Subsection 6.1. This asymptotic series becomes invalid as the thread becomes sufficiently thin. When this happens, we derive asymptotic solutions for two canonical problems. For the first canonical problem, in Subsection 6.2, we consider an example with the initial minimum bounded away from the pulled end. This example illustrates how one can determine the higher-order corrections to the solution of the obstacle problem discussed above that are essential to represent the solution in Eulerian coordinates and to determine the total extension. For the second canonical problem, in Subsection 6.3, we consider the case in which the initial minimum is at the pulled end. We show that the pinching at the pulled end is highly localized. Throughout this section, we will assume that the initial profile is symmetric about  $\xi = 0$ , so that we can apply the symmetry condition  $\partial_\xi(s_0 - s) = 0$  at  $\xi = 0$ .

### 6.1. Inertial Corrections Before the Thread becomes Asymptotically Thin

When the width of the thread is  $O(1)$ , the inertial terms give a small correction to the inertialess solution  $s = s_0(\xi) - \tau$ . This correction can be found by performing a straightforward perturbation analysis to obtain

$$s(\xi, \tau) = s_0(\xi) - \tau + \bar{R} \int_\xi^1 \int_0^{\xi'} \frac{1}{[s_0(\xi'') - \tau]^2} d\xi'' d\xi'. \quad (6.1)$$

Note that (2.21) and the initial condition (2.18) imply that  $s_\tau = 0$  at  $\tau = 0$ . Therefore, the solution (6.1) does not match the initial condition as  $\tau \rightarrow 0$ . This implies that there is an initial temporal adjustment region of width  $\tau = O(\tilde{R})$  over which the solution rapidly adjusts from the initial condition to match (6.1).

As discussed in Section 5, the inertial terms will become highly significant when the thread becomes sufficiently thin. When this occurs it is straightforward to check that the asymptotic ordering in (6.1) breaks down and alternative asymptotic approaches are required. In the following two subsections we describe the alternative asymptotic methods.

### 6.2. *Initial Minimum Located Away From End Points*

In this section, we consider how inertia affects the dynamics when the initial minimum is not at one of the end points of the thread. For simplicity, we consider the case in which the thread is symmetric around  $\xi = 0$  (or  $x = 0$  in the Eulerian coordinates). We also restrict our attention to the case in which the initial cross-sectional area profile of the thread,  $s_0(\xi)$ , is convex and has a single local minimum at  $\xi = 0$ .

To perform the formal asymptotic analysis, we show that the solution has different behaviour in three different regions. First, there is the necking region in which  $s = O(R)$ . Second, there is the outer region in which  $s = O(1)$ . Third, there is a thin region that connects the necking region and the outer region that we refer to as the transition region. In order to determine the solution, one must match the transition region with the necking and outer regions. In Figure 5, we plot a schematic of the different solution regions in the  $(\xi, \tau)$ -plane.

Equation (2.21) has three terms: the inertial term,  $\tilde{R}s_\tau$ , and two terms that arise from the stress, namely,  $s^2s_{\xi\xi}$  and  $s^2s_0\xi\xi$ . In the necking region, the cross-sectional area is small, so  $s_0 \gg s$  and generically  $s_0\xi\xi \gg s_{\xi\xi}$ . Therefore, the leading-order balance is

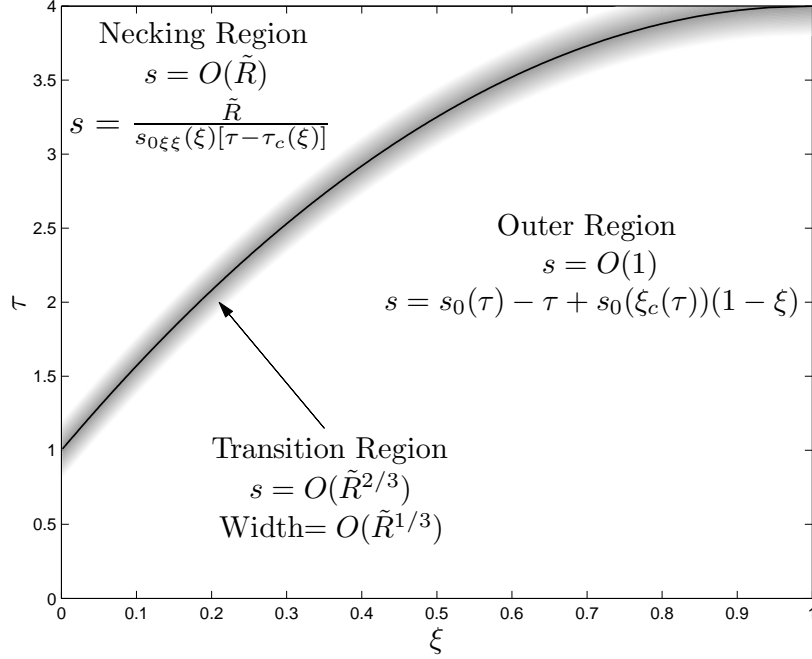


FIGURE 5. Schematic illustrating the asymptotic size and leading-order form of the solution in various regions of the  $(\xi, \tau)$  plane. The transition layer is located in a region of width  $O(\tilde{R}^{1/3})$  (shaded in grey) around  $\xi = \xi_c(\tau)$ . The function  $\xi = \xi_c(\tau)$  is plotted as a solid curve. Our analysis also makes use of the inverse function of  $\xi_c(\tau)$  which we denote as  $\tau_c(\xi)$  and is therefore also represented by the solid curve.

between the inertial term and the  $s^2 s_0 \xi \xi$  term. In the outer region,  $s = O(1)$ , and so the inertial terms are negligible and the leading-order balance is between the  $s^2 s_0 \xi \xi$  term and the  $s^2 s \xi \xi$  term. In the transition layer, we expect a transition from one type of balance to the other and so we expect all three terms to play a role. We begin by considering the transition layer.

### 6.2.1. Transition region

At leading order, we denote the location of the transition region as  $\xi = \xi_c(\tau)$ . We will determine  $\xi_c(\tau)$  later by matching with the other regions.

A standard scaling argument shows that one can obtain a balance between the three

terms if one chooses  $\xi - \xi_c(\tau) \sim \tilde{R}^{1/3}$  and  $s \sim \tilde{R}^{2/3}$ . We therefore introduce the following new variables

$$\eta = \frac{[\xi - \xi_c(\tau)]}{\tilde{R}^{1/3}K(\tau)} \quad \text{and} \quad s = \frac{\tilde{R}^{2/3}P}{Q(\tau)} \quad (6.2)$$

where  $K$  and  $Q$  are functions of  $\tau$  that are chosen to simplify the resulting differential equation and are given by

$$K = 2^{2/3} \left[ \dot{\xi}_c(\tau) \right]^{1/3} [s_{0\xi\xi}(\xi_c(\tau))]^{-2/3} \quad \text{and} \quad Q = 2^{-1/3} \left[ \dot{\xi}_c(\tau) \right]^{-2/3} [s_{0\xi\xi}(\xi_c(\tau))]^{1/3}. \quad (6.3)$$

Substituting into (2.21) and taking the leading-order terms in  $\tilde{R}$ , we obtain

$$P_\eta = P^2(2 - P_{\eta\eta}). \quad (6.4)$$

Dividing by  $P^2$  and integrating gives

$$P_\eta = 2(\eta - D_1(\tau)) + P^{-1} \quad (6.5)$$

where  $D_1(\tau)$  is a function of  $\tau$  that arises from the integration. Equation (6.5) represents the solution in a thin transition region layer that must be matched to the solutions on either side of the region. These matching conditions must be applied at  $\eta \rightarrow \pm\infty$ . Since this system is invariant under translations in  $\eta$ , we can set  $D_1 = 0$ . Then, (6.5) can be solved in implicit form in terms of Airy functions:

$$\eta = \frac{\text{Ai}'(\eta^2 - P) + C(\tau)\text{Bi}'(\eta^2 - P)}{\text{Ai}(\eta^2 - P) + C(\tau)\text{Bi}(\eta^2 - P)} \quad (6.6)$$

where  $C(\tau)$  is a function of  $\tau$  that arises from the integration and must be determined by matching.

### 6.2.2. Necking region

We now turn our attention to the necking region given by  $\xi < \xi_c(\tau)$  and  $\xi_c(\tau) - \xi \gg \tilde{R}^{1/3}$ . In this region, (2.21) can be approximated by

$$\tilde{R}s_\tau = -s^2 s_{0\xi\xi}(\xi). \quad (6.7)$$

This can be integrated with respect to time to give

$$s = \frac{\tilde{R}}{s_{0\xi\xi}(\xi)\tau + D(\xi)} \quad (6.8)$$

where  $D(\xi)$  is a function of  $\xi$  that arises from the integration and must be determined by matching.

### 6.2.3. Outer region

In the outer region, in which  $\xi > \xi_c(\tau)$  and  $\xi - \xi_c(\tau) \gg \tilde{R}^{1/3}$ ,  $s(\xi, \tau)$  is  $O(1)$ . We consider an asymptotic series of the form

$$s = s^{(0)} + \tilde{R}^{1/3}s^{(1)} + \tilde{R}^{2/3}s^{(2)} + \tilde{R}s^{(3)} + \dots \quad (6.9)$$

Substitution in (2.21) and using the boundary condition at  $\xi = 1$ , we obtain

$$\begin{aligned} s = s_0(\xi) - \tau + \left[ m^{(0)} + \tilde{R}^{1/3}m^{(1)} + \tilde{R}^{2/3}m^{(2)} + \tilde{R}m^{(3)} \right] (1 - \xi) \\ + \tilde{R} \int_{\xi}^1 \frac{[(1 - \xi')\dot{m}^{(0)} - 1](\xi' - \xi)}{[s_0(\xi') - \tau + (1 - \xi')m^{(0)}]^2} d\xi' \end{aligned} \quad (6.10)$$

where  $m^{(0)}, \dots, m^{(3)}$  are functions of  $\tau$  that arise from integration and must be determined by matching.

### 6.2.4. Matching necking and transition regions

In order to match the solutions obtained in the necking and transition regions, we first rewrite the solution in the necking region (6.8) in terms of the variables in the transition region (6.2) to obtain

$$P = \tilde{R}^{-2/3}Qs(\xi, \tau) = \frac{\tilde{R}^{1/3}Q}{[s_{0\xi\xi}\tau + D(\xi)]} \quad (6.11)$$

where  $\xi$  is given by

$$\xi = \xi_c(\tau) + \tilde{R}^{1/3}K\eta. \quad (6.12)$$

We now define the function  $\tau_c(\xi)$  such that  $\tau_c(\xi_c(\tau)) = \tau$ . That is,  $\tau_c(\xi)$  is the inverse function of  $\xi_c(\tau)$ . We now express the term involving  $\tau$  in (6.11) as

$$\begin{aligned}\tau &= \tau_c(\xi_c(\tau)) = \tau_c\left(\xi - \tilde{R}^{1/3}K\eta\right) \\ &= \tau_c(\xi) - \tilde{R}^{1/3}K\tau_{c\xi}(\xi)\eta + O(\tilde{R}^{2/3})\end{aligned}\tag{6.13}$$

to obtain

$$P = \frac{\tilde{R}^{1/3}Q}{D(\xi) + s_{0\xi\xi}(\xi)\tau_c(\xi) - \tilde{R}^{1/3}s_{0\xi\xi}(\xi)K\tau_{c\xi}(x)\eta} + O(\tilde{R}^{2/3}).\tag{6.14}$$

By examining (6.5), one can see that the solution in the transition layer (6.6) has two possible asymptotic behaviors as  $\eta \rightarrow -\infty$ , namely,  $P \sim \eta^2$ , or  $P \sim -1/(2\eta)$ . The form of the solution in the necking region (6.14) means that matching can only be consistently performed if two conditions are met. First, the transition region must have asymptotic behavior  $P \sim -1/(2\eta)$  as  $\eta \rightarrow -\infty$ . Letting  $\eta \rightarrow -\infty$  in (6.6) and noting that  $\text{Ai}(x)/\text{Bi}(x) \rightarrow 0$ ,  $\text{Ai}'(x)/\text{Bi}'(x) \rightarrow 0$ , and  $\text{Bi}'(x)/\text{Bi}(x) \sim \sqrt{x}$  as  $x \rightarrow \infty$ , we see that this can only occur if

$$C(\tau) = 0.\tag{6.15}$$

Second, the function  $D(\xi)$  must be chosen so that

$$D(\xi) = -s_{0\xi\xi}(\xi)\tau_c(\xi).\tag{6.16}$$

Matching also requires

$$\frac{Q}{s_{0\xi\xi}(\xi)K\tau_c(\xi)} = \frac{1}{2}.\tag{6.17}$$

Using (6.3), this can be reduced to  $\dot{\xi}_c(\tau)\tau_{c\xi}(\xi) = 1$ , but, at leading order, this is automatically satisfied since  $\xi_c$  and  $\tau_c$  are inverse functions and  $\tau_{c\xi}(\xi) = \tau_{c\xi}\left(\xi_c(\tau) + O(\tilde{R}^{1/3})\right) = \tau_{c\xi}(\xi_c(\tau)) + O(\tilde{R}^{1/3})$ .

Hence, the solution in the necking region is given by

$$s = \frac{\tilde{R}}{s_{0\xi\xi}(\xi)[\tau - \tau_c(\xi)]},\tag{6.18}$$

and the solution in the transition region can be obtained by substituting  $C(\tau) = 0$  into (6.6) to obtain

$$P = \eta^2 - f^{-1}(\eta) \quad (6.19)$$

where  $f(x) = \text{Ai}'(x)/\text{Ai}(x)$  and the inverse function  $f^{-1}(x)$  selects the root in the range  $(Z_0, \infty)$  where  $Z_0 = -2.338107410\dots$  is the first zero of the Airy function. We note that when rewritten in the original variables, (6.19) is given by

$$s = \frac{(\xi - \xi_c)^2 s_{0\xi\xi}(\xi_c)}{2} - \frac{\tilde{R}^{2/3}}{Q(\tau)} f^{-1}\left(\frac{(\xi - \xi_c)}{\tilde{R}^{1/3} K(\tau)}\right). \quad (6.20)$$

### 6.2.5. Matching outer and transition regions

Equation (6.19) has the asymptotic form

$$P \sim \eta^2 + Z_0 - \eta^{-1} \quad \text{as } \eta \rightarrow \infty, \quad (6.21)$$

and this must be matched with the solution in the outer region (6.10) as  $\xi \rightarrow \xi_c+$ . We rewrite the solution in the outer region (6.10) in terms of the variables in the transition region

$$\begin{aligned} P = & \tilde{R}^{-2/3} Q \left[ s_0(\xi_c + \tilde{R}^{1/3} K\eta) - \tau + (1 - \xi_c)m^{(0)} \right] + \tilde{R}^{-1/3} Q \left[ (1 - \xi_c)m^{(1)} - K\eta m^{(0)} \right] \\ & + Q \left[ (1 - \xi_c)m^{(2)} - K\eta m^{(1)} \right] + \tilde{R}^{1/3} Q \left[ (1 - \xi_c)m^{(3)} - K\eta m^{(2)} \right] \\ & + \tilde{R} Q K^2 \int_{\eta}^{\frac{(1-\xi_c)}{\tilde{R}^{1/3} K}} \frac{(\eta' - \eta) \left[ (1 - \xi_c)\dot{m}^{(0)} - 1 - \tilde{R}^{1/3} K\eta' \dot{m}^{(0)} \right]}{\left[ s_0(\xi_c + \tilde{R}^{1/3} K\eta') - \tau + (1 - \xi_c - \tilde{R}^{1/3} K\eta')m^{(0)} \right]^2} d\eta'. \end{aligned} \quad (6.22)$$

Expanding  $s^{(0)}$  near  $\xi = \xi_c$ , we obtain

$$s^{(0)} = s_0(\xi_c) - \tau + (1 - \xi_c)m^{(0)} + (\xi - \xi_c) \left[ s_{0\xi}(\xi_c) - m^{(0)} \right] + O((\xi - \xi_c)^2). \quad (6.23)$$

For compatibility with (6.2), it is necessary that

$$s_0(\xi_c) - \tau + (1 - \xi_c)m^{(0)} = 0. \quad (6.24)$$

$$s_{0\xi}(\xi_c) - m^{(0)} = 0. \quad (6.25)$$

After substituting (6.24) and (6.25) into (6.22), evaluating the integral, and taking the leading orders in  $\tilde{R}$ , we obtain

$$P = \tilde{R}^{-1/3} Q(1 - \xi_c) m^{(1)} + Q \left[ (1 - \xi_c) m^{(2)} - K \eta m^{(1)} + \frac{1}{2} K^2 \eta^2 s_{0\xi\xi}(\xi_c) \right] - \frac{2Q\dot{m}^{(0)}}{s_{0\xi\xi}^2(\xi_c) K \eta}. \quad (6.26)$$

Matching with (6.21) at  $O(\tilde{R}^{-1/3})$ , we see that  $m^{(1)} = 0$ . At  $O(1)$ , using (6.3), we obtain

$$\eta^2 + Z_0 - \eta^{-1} \equiv \eta^2 + Q(1 - \xi_c) m^{(2)} - \frac{\dot{m}^{(0)}}{s_{0\xi\xi}(\xi_c) \xi_c} \eta^{-1}. \quad (6.27)$$

By differentiating (6.25) with respect to  $\tau$ , we obtain  $\dot{m}^{(0)} = s_{0\xi\xi}(\xi_c) \dot{\xi}_c$ , and so the  $\eta^{-1}$  term automatically matches. Therefore, the only condition for matching is

$$m^{(2)} = Z_0(1 - \xi_c)^{-1} 2^{1/3} \left[ \dot{\xi}_c(\tau) \right]^{2/3} [s_{0\xi\xi}(\xi_c(\tau))]^{-1/3}. \quad (6.28)$$

We can combine the solutions in different regions and construct a uniform asymptotic solution, given by

$$s = \frac{\tilde{R}}{s_{0\xi\xi}(\xi)} \left[ \frac{1}{\tau - \tau_c(\xi)} + \frac{\dot{\xi}_c(\tau)}{\xi - \xi_c} \right] H(\xi_c - \xi) + \frac{(\xi - \xi_c)^2 s_{0\xi\xi}(\xi_c)}{2} - \frac{\tilde{R}^{2/3}}{Q(\tau)} f^{-1} \left( \frac{(\xi - \xi_c)}{\tilde{R}^{1/3} K(\tau)} \right) + \left[ s_0(\xi) - \tau + (1 - \xi) s_{0\xi}(\xi_c) - \frac{(\xi - \xi_c)^2 s_{0\xi\xi}(\xi_c)}{2} \right] H(\xi - \xi_c) \quad (6.29)$$

where  $H(\cdot)$  is the Heaviside function.

### 6.2.6. Total extension

In the above Subsection, we have determined the cross-sectional area,  $s$ , of a given fluid element as a function of the Lagrangian variable  $\xi$ . However, in order to determine the location of the fluid element, one must compute the extension integral (2.13). In this Subsection, we use this integral to determine the location of the pulled end. The integral can be broken into the contributions from each of the three regions: necking, transition, and outer. The length of the outer region is  $O(1)$ , and in this region, the thread has cross-sectional area of  $O(1)$ . Hence, the contribution from the outer region

to (2.13) is  $O(1)$ . The length of the transition region is  $O(\tilde{R}^{1/3})$ , and in this region, the thread has cross-sectional area of  $O(\tilde{R}^{2/3})$ . Hence, the contribution from the transition region is  $O(\tilde{R}^{-1/3})$ . Finally, the length of the necking region is  $O(1)$ , and in this region, the thread has cross-sectional area of  $O(\tilde{R})$ . Hence, the contribution from the necking region is  $O(\tilde{R}^{-1})$ . Therefore, the leading-order contribution for the extension comes only from the necking region.

Using the leading-order expression for  $s$  in the necking region (6.18) and noting that  $\tilde{R} = IR$ , we obtain

$$X(1, \tau) = \frac{1}{R} \int_0^{\xi_c(\tau)} s_{0\xi\xi}(\xi) [\tau - \tau_c(\xi)] d\xi + O(R^{-1/3}). \quad (6.30)$$

Making the substitution  $\xi = \xi_c(\hat{\tau})$  and noting that  $\tau_c$  is the inverse of  $\xi_c$ , we obtain

$$X(1, \tau) = \frac{1}{R} \int_1^\tau s_{0\xi\xi}(\xi_c(\hat{\tau})) [\tau - \hat{\tau}] \dot{\xi}_c(\hat{\tau}) d\hat{\tau} + O(R^{-1/3}). \quad (6.31)$$

Integrating by parts and using the fact that  $s_{0\xi}(0) = 0$  gives

$$X(1, \tau) = \frac{1}{R} \int_1^\tau s_{0\xi}(\xi_c(\hat{\tau})) d\hat{\tau} + O(R^{-1/3}). \quad (6.32)$$

### 6.2.7. Example with exact solution

Here, we illustrate our solution method using a set of initial profiles for which one can obtain simple analytical solutions. We consider initial profiles of the form  $A_0(x) = \sec^2(\kappa x)$  where  $0 < \kappa < \pi/2$ . Using (2.6), we obtain

$$\xi = \frac{\tan \kappa x}{\tan \kappa}. \quad (6.33)$$

Hence, rewriting the initial profile  $A_0(x)$  in terms of the Lagrangian variable  $\xi$  gives

$$s_0(\xi) = 1 + k\xi^2 \quad (6.34)$$

where  $k = \tan^2 \kappa$ .

Using the profile (6.34), one can solve (5.4) to obtain an explicit expression for  $\xi_c(\tau)$

given by

$$\xi_c(\tau) = 1 - \sqrt{1 + k^{-1}(1 - \tau)}. \quad (6.35)$$

The inverse of  $\xi_c(\tau)$  is given by

$$\tau_c(\xi) = 1 - k\xi^2 + 2k\xi. \quad (6.36)$$

Having determined these functions, it is then straightforward to obtain the leading-order solutions in the outer, necking, and transition regions. These are given by

$$s(\xi, \tau) = 1 + k\xi^2 + 2(1 - \xi)k \left[ 1 - \sqrt{1 + k^{-1}(1 - \tau)} \right], \quad (6.37)$$

$$s(\xi, \tau) = \frac{\tilde{R}}{2k[\tau - 1 + k\xi^2 - 2k\xi]}, \quad (6.38)$$

and

$$s(\xi, \tau) = k \left[ \xi - 1 + \sqrt{1 + k^{-1}(1 - \tau)} \right]^2 - \frac{\tilde{R}^{2/3}}{2^{2/3}k[1 + k^{-1}(1 - \tau)]^{1/3}} \times \quad (6.39)$$

$$f^{-1} \left( \frac{2^{1/3}k[1 + k^{-1}(1 - \tau)]^{1/6} \left[ \xi - 1 + \sqrt{1 + k^{-1}(1 - \tau)} \right]}{\tilde{R}^{1/3}} \right), \quad (6.40)$$

respectively. The leading-order total extension also can be computed explicitly and is given by

$$X(1, \tau) = \frac{2k^2}{3\tilde{R}} \left[ 3k^{-1}(\tau - 1) + 2 \left[ 1 + k^{-1}(1 - \tau) \right]^{3/2} - 2 \right]. \quad (6.41)$$

In Figure 6, we plot the asymptotic and numerical solutions for two different Reynolds numbers. They show good agreement for  $\tilde{R} = 10^{-3}$  and excellent agreement for  $\tilde{R} = 10^{-4}$ . The total extension is shown as a function of  $\tilde{R}$  in Figure 7 at the time close to pinching. As  $\tilde{R}$  decreases, the agreement between the asymptotic and numerical solutions becomes better.

### 6.3. Initial Minimum Located at End Point

Assume that the minimum of the initial cross-sectional area,  $s_0$ , is located at one of the end points, then, without loss of generality, we can assume that the initial minimum

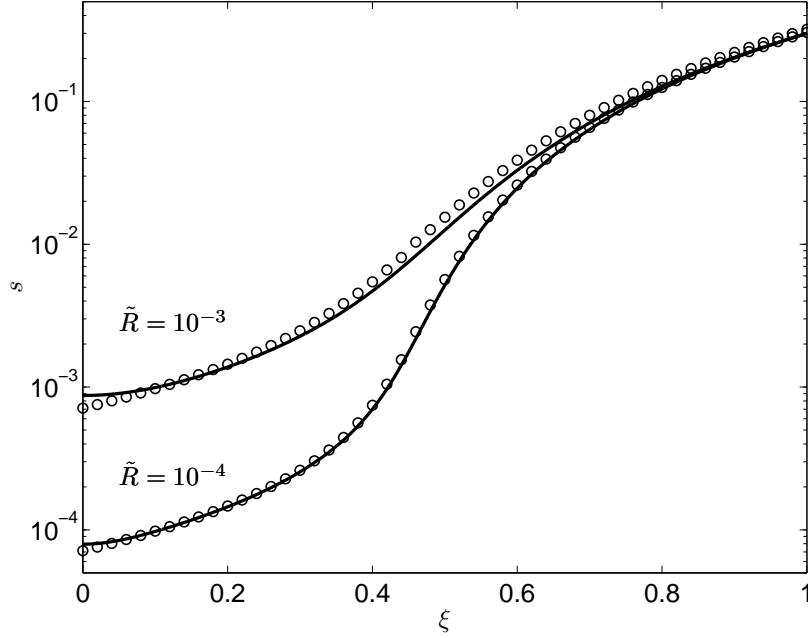


FIGURE 6. The cross-sectional areas for  $\tilde{R} = 10^{-3}$  and  $10^{-4}$  are plotted against the Lagrangian variable  $\xi$  at  $\tau = 1.7$ . The solid curves represent the numerical solutions and the circles represent the uniform asymptotic solution (6.29). The initial condition is given by (6.34) with  $k = 1$ .

is located at  $\xi = 1$ . The initial minimum cross-section is defined to be unity and so  $s_0(1) = 1$ .

We expect inertia to become important only when  $s \ll 1$ . So initially, the leading-order behavior is  $s(\xi, \tau) = s_0(\xi) - \tau$ . This solution breaks down when  $\tau$  approaches unity at which time the cross-sectional area,  $s$ , becomes small near  $\xi = 1$ . It seems natural to use matched asymptotic expansion methods to solve this problem [with a boundary layer](#) in which  $s$ ,  $1 - \xi$ , and  $1 - \tau$  are all small. Using the governing equation (2.21) with boundary condition (2.22) and assuming a matching condition in which  $s_c$  is matched with the outer solution, one is naturally led to choose variables  $1 - \xi = \tilde{R}\bar{\xi}$ ,  $1 - \tau = \tilde{R}\bar{\tau}$ , and  $s = \tilde{R}\bar{s}$ . Using these variables, the leading-order governing equation is given by

$$\bar{s}_{\bar{\tau}} = -\bar{s}^2 \bar{s}_{\bar{\xi}\bar{\xi}}. \quad (6.42)$$

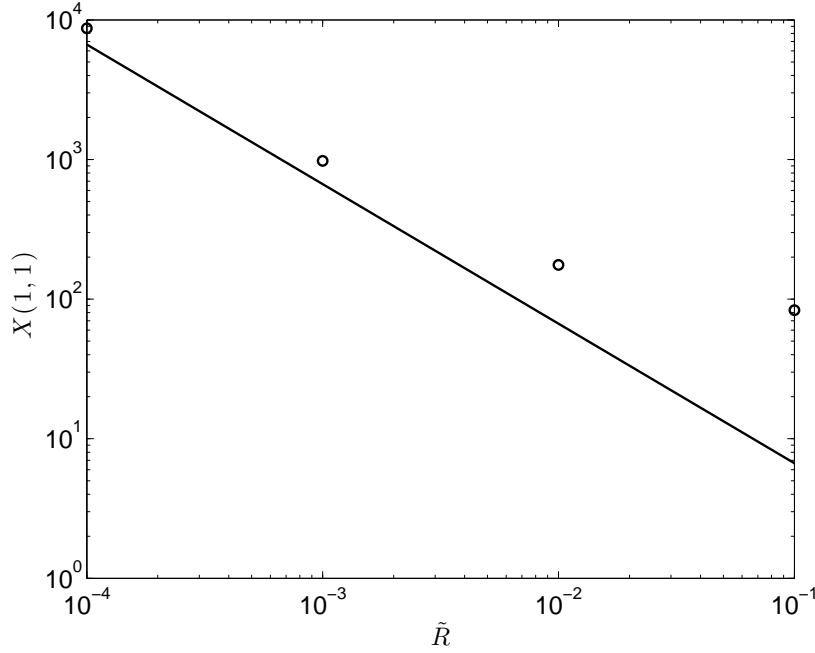


FIGURE 7. The total extension near pinching is plotted against  $\tilde{R}$ . The numerical solution is shown as circles and the asymptotic solution is shown as a straight solid line. The initial condition is given by (6.34) with  $k = 1$ .

Equation (6.42) must satisfy,  $\bar{s} = \bar{\tau}$  at  $\bar{\xi} = 0$  and a matching condition as  $\bar{\xi} \rightarrow \infty$ . Equation (6.42) also requires a condition as  $\bar{\tau} \rightarrow -\infty$ , which must be obtained by matching with (6.1), although it is possible that an intermediate structure may be required for the matching.

We note that (6.42) can be transformed into a linear diffusion equation using a procedure given by Blumen & Kumei (1980). However, under the transformation, the boundary conditions become sufficiently complicated that they have prevented us from obtaining an analytical solution. Nevertheless, we have made progress by introducing the variables

$$s(\xi, \tau) = s_0(\xi) - 1 + (1 - \tau)a(\zeta, T) \quad (6.43)$$

where

$$\zeta = \frac{(1 - \xi)\tilde{R}^{1/2}}{(1 - \tau)^{3/2}} \quad \text{and} \quad T = -\ln \left[ \frac{1 - \tau}{\tilde{R}} \right]. \quad (6.44)$$

Here  $\zeta$  represents a scaled distance from the pulled end and  $T$  is a time-like variable that tends to infinity as the thread approaches pinching, that is, as  $\tau \rightarrow 1$ . We note that these scalings imply that  $s = O(\tilde{R})$ ,  $1 - \tau = O(\tilde{R})$ , and  $1 - \xi = O(\tilde{R})$ . As we will see below, this choice of variables allows us to obtain the form of the solution close to the pinched end.

Substituting into (2.21), we obtain

$$2a_T - 2a + 3\zeta a_\zeta = 2 \left[ a + \frac{s_0 \left( 1 - \tilde{R} e^{-3T/2} \zeta \right) - 1}{\tilde{R} e^{-T}} \right]^2 a_{\zeta\zeta}. \quad (6.45)$$

The boundary condition (2.22) becomes

$$a = 1 \quad \text{at} \quad \zeta = 0. \quad (6.46)$$

The symmetry condition  $\partial_\xi(s_0 - s) = 0$  at  $\xi = 0$  becomes

$$a_\zeta = 0 \quad \text{at} \quad \zeta = \tilde{R}^{-1} e^{3T/2}. \quad (6.47)$$

From matching with  $s = s_0(\xi) - \tau$ , which is valid for  $1 - \tau \gg \tilde{R}$ , we obtain

$$a = 1 \quad \text{as} \quad T \rightarrow -\infty. \quad (6.48)$$

Of particular interest is what happens very close to pinching, that is, as  $T \rightarrow \infty$ . We first use the mean value theorem and the fact that  $s_0(1) = 1$  to obtain

$$2a_T - 2a + 3\zeta a_\zeta = 2 \left[ a + s_{0\xi}(\alpha) e^{-T/2} \zeta \right]^2 a_{\zeta\zeta}, \quad (6.49)$$

where  $1 - \tilde{R} e^{-3T/2} \zeta < \alpha < 1$ . For  $\zeta = O(1)$  and  $T \rightarrow \infty$ , (6.49) reduces to an ordinary differential equation given by

$$-2a + 3\zeta a_\zeta = 2a^2 a_{\zeta\zeta}. \quad (6.50)$$

The boundary condition  $a = 1$  at  $\zeta = 0$  can be applied, but the boundary condition at  $\zeta = \tilde{R}^{-1} e^{3T/2}$  cannot be directly applied since it is unclear whether the term  $2a_T$  and the term involving  $e^{-T/2} \zeta$  are important at this large value of  $\zeta$ .

A straightforward analysis of (6.50) shows that there are three types of solutions. First, there is an infinite family of solutions that have a singularity at a finite value of  $\zeta$ . Such solutions are clearly unphysical and we therefore do not need to consider them. Second, there is an infinite family of solutions that have the property that  $a \rightarrow \zeta(\ln \zeta)^{1/2}$  as  $\zeta \rightarrow \infty$ . Finally, there is a special solution that divides the two solution types. This solution is given by

$$\zeta = \frac{2}{3}(a-1) \left( a + \frac{1}{2} \right)^{1/2}. \quad (6.51)$$

and has the property that  $a$  is proportional to  $\zeta^{2/3}$  as  $\zeta \rightarrow \infty$ . In deriving (6.50) from (6.49), we initially assumed that  $\zeta = O(1)$ . This ensured that the  $a_T$  and  $e^{-T/2}\zeta$  terms in (6.49) are small. However, the solution (6.51) is a valid approximation to (6.49) beyond the range  $\zeta = O(1)$ . By comparing the terms on the left-hand side of (6.49), one can see that the  $a_T$  term will be negligible if  $\zeta \ll e^{3T/2}$ . For the two remaining solution types, one can readily check that the  $2a$  and  $3\zeta a_\zeta$  terms on the left-hand side of (6.49) are always larger than the terms on the right-hand side involving  $e^{-T/2}\zeta$ . Therefore, both solution types satisfy (6.49) even for large values of  $\zeta$  that are  $o(e^{3T/2})$ . However, for large values of  $\zeta$  that are smaller than  $e^{3T/2}$ , one can show that the family of solutions with asymptotic form  $a \sim \zeta(\ln \zeta)^{1/2}$  correspond to solutions in which  $s_\xi$  becomes arbitrarily large and negative. We therefore conclude that the solution (6.50) is given implicitly by (6.51). In the original variables, for  $(1-\xi) \ll \tilde{R}$ , the solution near pinching is given by

$$s(\xi, \tau) = (1-\tau)a \left( \frac{(1-\xi)\tilde{R}^{1/2}}{(1-\tau)^{3/2}} \right) \quad \text{as} \quad \tau \rightarrow 1, \quad (6.52)$$

with  $a$  given by (6.51). For  $\zeta = O(e^{3T/2})$  up to the boundary at  $\zeta = \tilde{R}^{-1}e^{3T/2}$ , one needs to solve the full parabolic partial differential equation (6.45), which does not readily admit analytical solutions. We note that (6.52) corresponds to a similarity solution of (6.42) in the form  $\bar{s} = \bar{\tau}a(\bar{\xi}/\bar{\tau}^{3/2})$ .

## 7. Discussion and Physical Interpretation

In this paper, we have obtained asymptotic solutions of the problem of a viscous thread that is pulled at its ends by an imposed fixed force at low Reynolds numbers. We have shown that the inertial effects are crucial in determining the dynamics of the stretching. Furthermore, we have shown that the leading-order solution in Lagrangian coordinates can be obtained by solving an obstacle problem. However, in Eulerian coordinates, one must go beyond the leading order in the necking region in order to determine the extension integral. We have considered two canonical problems that exhibit completely different behaviour. In both cases, we derived solutions by using asymptotic methods. We showed that the inclusion of inertia implies that the total extension remains finite, contrary to the inertialess case.

In order to understand the physical mechanism by which inertia prevents pinching, we integrate (2.15) and obtain

$$s^2 v_\xi = 1 - \tilde{R} \frac{\partial}{\partial \tau} \int_\xi^1 v d\hat{\xi}. \quad (7.1)$$

On the left-hand side of the equation is the viscous force which is responsible for stretching the thread. The right-hand side contains the pulling force (normalized to be one) and the inertial terms. This equation shows how the effective pulling force, which we define to be  $1 - \tilde{R} \frac{\partial}{\partial \tau} \int_\xi^1 v d\hat{\xi}$ , is reduced by inertia. The quantity  $\int_\xi^1 v d\hat{\xi}$ , which represents the momentum of the thread between  $\xi$  and 1. Initially  $\int_\xi^1 v d\hat{\xi} = O(1)$  and since  $\tilde{R}$  is small, the force reduction due to the motion of the thread is small. However, when the necking region forms, the accelerations can become  $O(\tilde{R}^{-1})$  and so the force reduction term can become significant. This is true for points in the vicinity and to the left of the necking region. However, for points near the end of the thread ( $\xi = 1$ ), the force reduction is small. This is because, the force is prescribed at the end of the thread, and so no force reduction can occur there. Our solution implies that the inertial terms reduce the effective

stretching force to  $O(\tilde{R})$  when the necking region forms and this force reduction prevents pinching.

Finally, we address the question of the validity of neglecting the surface tension terms in (2.16). We note that the only times when surface tension can possibly be important are those times when the thread is close to pinching. We first consider the case in which the initial minimum is at one of the end points of the thread. By examining the local solution (6.52) as pinching is approached, we see that the term  $s_\tau$  in (2.16) is order unity, whereas the term  $\lambda s^{1/2}$  is of  $O(\lambda(1-\tau)^{1/2})$ . Therefore  $s_\tau \gg \lambda s^{1/2}$  and surface tension in (2.16) can be neglected.

We now consider the case in which the initial minimum is bounded away from the end points. Prior to the formation of the necking, outer, and transition regions, the thread has cross-sectional area of  $O(1)$  and so surface tension can be neglected. However, following the formation of the three regions, one must consider each of the regions separately. In the outer region,  $s = O(1)$  and the operator  $\partial_\tau = O(1)$ , and therefore, the term  $s_\tau$  in (2.16) is  $O(1)$ . On the other hand, the term  $\lambda s^{1/2}$  is of  $O(\lambda)$ . Since  $\lambda \ll 1$ , we conclude that  $s_\tau \gg \lambda s^{1/2}$ . In the transition region,  $s = O(\tilde{R}^{2/3})$  and  $\partial_\tau = O(\tilde{R}^{-1/3})$ . Therefore,  $s_\tau = O(\tilde{R}^{1/3})$  and  $\lambda s^{1/2} = O(\lambda \tilde{R}^{1/3})$ , and hence,  $s_\tau \gg \lambda s^{1/2}$ . In the necking region,  $s = O(\tilde{R})$ ,  $\partial_\xi = O(1)$ , and  $\partial_\tau = O(1)$ . Therefore,

$$\tilde{R} \left[ \frac{s_\tau}{s^2} \right]_\tau = O(1) \quad \text{and} \quad \left[ \lambda s^{1/2} \right]_{\xi\xi} = O(\lambda \tilde{R}^{1/2}), \quad (7.2)$$

and hence,

$$\tilde{R} \left[ \frac{s_\tau}{s^2} \right]_\tau \gg \left[ \lambda s^{1/2} \right]_{\xi\xi}. \quad (7.3)$$

Thus, in each of the three regions, the surface tension term is negligible compared with the dominant term in that region. Hence, our neglect of the surface tension terms throughout the extension process is well justified.

Under the long-wavelength approximation, the thread will pinch at the pulled end. However, as the pinching event is approached, the long-wavelength approximation breaks down and the problem becomes two dimensional. In this case, the exact details of the pinching process will depend on the nature of the boundary conditions at the pulled end. The analysis for this process is beyond the scope of this paper and will be addressed in future work.

**Acknowledgment** The authors would like to thank an anonymous referee for a number of suggestions that helped us to improve the manuscript. The authors acknowledge financial support from the Research Grants Council of the Hong Kong Special Administrative Region, China [CityU 102909] (JJW), NSERC and MITACS (HH), and NSF (RMM).

#### REFERENCES

- BLUMAN, G. & KUMEI, S. 1980 On a remarkable nonlinear diffusion equation *J. Math. Phys.* **21**, 1019–1023.
- BRADSHAW-HAJEK, B.H., STOKES, Y.M. & TUCK, E.O. 2004 Computation of extensional flow of slender viscous drops by a one-dimensional Eulerian method. *SIAM J. Appl. Math.* **67**, 1166–1182.
- EGGERS, J. 2005 Drop formation - an overview. *Z. Angew. Math. Mech.* **85**, 400–410.
- FITT, A.D., FURUSAWA, K., MONRO, T.M. & PLEASE, C.P. 2001 Modeling the fabrication of hollow fibers: Capillary drawing. *J. Lightwave Technologies* **19**, 1924–1931.
- FOREST, M.G., ZHOU, H. & WANG, Q. 2000 Thermotropic liquid crystalline polymer fibers. *SIAM J. Appl. Math.* **60**, 1177–1204.
- GALLACCHI, R., KOLSCH, S., KNEPPE, H. & MEIXNER, A.J. 2001 Well-shaped fibre tips by pulling with a foil heater. *J. Microscopy* **202**, 182–187.
- HUANG, H., MIURA, R.M., IRELAND, W. & PUIL, E. 2003 Heat-induced stretching of a glass

- tube under tension: Application to glass microelectrodes. *SIAM J. Appl. Math.* **63**, 1499–1519.
- HUANG, H., WYLIE, J.J., MIURA, R.M. & HOWELL, P.D. 2007 On the formation of glass microelectrodes. *SIAM J. Appl. Math.* **67**, 630–666.
- KAYE, A. 1991 Convective coordinates and elongational flow. *J. Non-Newtonian Fluid Mech.* **40**, 55–77.
- MATTA, J.E. & TYTUS, R.P. 1990 Liquid stretching using a falling cylinder. *J. Non-Newtonian Fluid Mech.*, **35**, 215–229.
- STOKES, Y.M. & TUCK, E.O. 2004 The role of inertia in extensional fall of a viscous drop. *J. Fluid Mech.* **498**, 205–225.
- STOKES, Y.M., TUCK, E.O. & SCHWARTZ, L.W. 2000 Extensional fall of a very viscous fluid drop. *Q. J. Mech. Appl. Maths.* **53**, 565–582.
- WILSON, S.D.R. 1988 The slow dripping of a viscous fluid. *J. Fluid Mech.*, **190**, 561–570.
- WYLIE, J.J. & HUANG, H. 2007 Extensional flows with viscous heating. *J. Fluid Mech.*, **571**, 359–370.
- YIN, Z. & JALURIA, Y. 2000 Neck down and thermally induced defects in high-speed optical fiber drawing. *ASME J. Heat Transfer* **122**, 351–362.